Al-Nahrain Journal for Engineering Sciences **NJES** 27(1)118-123, 2024
http://doi.org/10.29194/NJES.27010118

Exploring the Potentials of Laser Induced Forward Transfer and Laser Annealing Processes for Synthesis/Printing of Silver Nanofilms on Quartz Substrates using Nd:YAG and CO_2 Laser Beams

Hanadi H. Altawil

Authors affiliations:
1) Mathematics, Computer & Natural Sciences Division of Ohio Dominican University, USA
altawilh@ohiodominican.edu

Paper History:

Received: 2nd March 2023

Revised: 9th May 2023

Accepted: 30th Jan. 2024

Abstract

Laser annealing represents a powerful method for tailoring the properties of silver nanofilms on quartz substrates, offering advantages in terms of precision, scalability, and functionalization. Continued research efforts are expected to deepen our understanding and broaden the applications of this promising technology in diverse fields. In this work, laser annealing of silver nanofilms deposited on quartz substrates was performed and investigated. RF CO_2 laser of variable power in the range 1–20 W with beam quality of 1.1 was used to anneal silver nanofilms. AFM analysis emphasized that nanocrystal sizes of 60 nm were obtained for silver nanofilms. Furthermore, the optimum absorbance peak occurred at about 449 nm for smaller film thickness. Thermal simulation and analysis of the annealing process were also conducted using COMSOL Multiphysics software. It was observed that optimal temperature of 729 K was achieved when 10 W laser power and 2 mm/s scanning speed were used to anneal 20 nm silver film thickness. Design of expert analysis was also used to better understand the laser annealing process of silver nanofilms since convolution of several process parameters affect the process output.

Keywords: Laser Annealing; Ag thin film; COMSOL Multiphysics, Design of Experiments

1. Introduction

Laser annealing of silver nanofilms on quartz substrates has garnered significant attention due to its potential applications in various fields such as optoelectronics, plasmonics, and sensors. This technique offers precise control over the properties of silver nanostructures, including morphology, crystallinity, and optical characteristics. Laser annealing has been shown to enable controlled growth of silver nanoparticles on quartz substrates, leading to enhanced optical properties and stability [1-3]. Studies have demonstrated that laser annealing influences the surface morphology and roughness of silver nanofilms, affecting their plasmonic behavior and sensitivity [4-7]. The optical properties of silver nanostructures can be tailored through laser annealing, optimizing their plasmonic resonances for applications in surface-enhanced spectroscopies [8,9]. Laser-induced annealing induces structural evolution and crystallinity changes in silver nanofilms, impacting their electronic and thermal conductivity [10-13]. Various fabrication techniques and process parameters have been explored to optimize laser annealing for silver nanofilms on quartz, balancing efficiency and quality [14,15]. The unique properties achieved through laser annealing make silver nanofilms on quartz substrates promising for applications in sensing platforms and integrated photonics [16-18]. Comparative studies highlight the advantages of laser annealing over conventional thermal annealing for silver nanofilms, emphasizing enhanced control and reproducibility [19,20]. Computational modeling and simulation approaches have been employed to elucidate the dynamics of laser-induced annealing on silver nanofilms, providing insights into process optimization [21,22]. Laser-annealed silver nanofilms exhibit improved stability and durability under harsh environmental conditions, crucial for practical applications [23]. Future research directions include exploring novel laser sources and advanced characterization techniques to further enhance the performance and functionality of silver nanofilms on quartz substrates [24-26]. This work investigates the effect of laser parameters on annealing of silver metallic thin films. The results could improve the knowledge on many applications concerning synthesis of metallic nanostructures and plasmonic applications in optoelectronics field. In this work, sputtering process was used for depositing silver nanofilm and RF CO_2 laser for annealing process was employed, then COMSOL Multiphysics software was used for simulate the thermal effect of the laser annealing of silver nanofilm that is not found in previous researches.

2. Experimental Work

Silver nanofilms of various thicknesses were synthesised via Laser Induced Forward Transfer

NJES is an **open access Journal** with **ISSN 2521-9154** and **eISSN 2521-9162**

process (LIFT). To prepare the silver nanofilm samples, quartz slides (from HMCL) of 15×15×1 mm dimensions were used as substrates. Nano Labs silver nano-paste with more than 75% concentration of silver nano-particle sizes (10-20 nm) was used as the donor layer in the LIFT process shown in Fig. 1(a). The quartz slides were cleaned with ethanol alcohol then dried in air. Silver nano-paste was filled onto the donor slide, which was irradiated, from the back side, by a Q-switch-pulsed Nd:YAG laser (TRUMPF-TruPulse 21, which has a 1064 nm wavelength, a total maximum power of 20 W, 15 J maximum pulse energy and a variable pulse duration 0.2-50 ms). The distance between the donor slide and receiving slide was kept at 6 mm. As a result, a small portion of the donor film is ejected forward by means of shock forming and ablation, resulting in the penetration of the ejected material onto the receiving slide. Bursts of pulses within 1 ms duration were used in the LIFT process. Furthermore, the laser pulse energy and number of pulses were varied within these process parameter values (3 J and 5 J, 10-50 pulses) respectively in order to produce different layer thicknesses of transferred silver particles onto the receiving slide.

The slides resulting from the LIFT process were, afterwards, mounted on the X-Y translation stage of the laser annealing (LA) system. The annealing process was performed using a CW RF-CO_2 laser beam as shown in Fig. 1(b). The laser source utilized in the LA process was (Coherent, C-20 CO_2 laser, which has a selectable wavelength from 9.3 to 10.6 µm, beam size of 1.8±0.2 mm, power range from 1-20 W and a beam quality M^2 ~ 1.1). During the LA process, the laser beam wavelength was set to 10.6 µm and had a practically Gaussian transverse mode and a diameter, after expansion and focusing, of 10 mm at the front side of the silver nanofilm surface. Based on initial screening experiments, it was decided to set the laser power and scanning speed to values of (10 W, 2 mm/s) respectively.

The processed samples were examined and characterised using a digital optical microscope (Olympus, BX-60). Furthermore, Angstrom Advanced AA2000 Combined Atomic Force Microscope (AFM) was used to characterise the surface morphology, nanostructure scales and calculate the layer thickness. Finally, the optical absorption spectra of the samples were examined using a (Metertech, SP-80001) Diffuse Reflectance Spectroscopy (DRS). The latter three characterisation methods were implemented for each sample before and after LA processing.

To get a deeper understanding of the process parameters on the resulting surface morphologies, COMSOL Multiphysics 5.4 simulation software was used to study the temperature distribution on the Silver nanofilm as a result of the LA process.

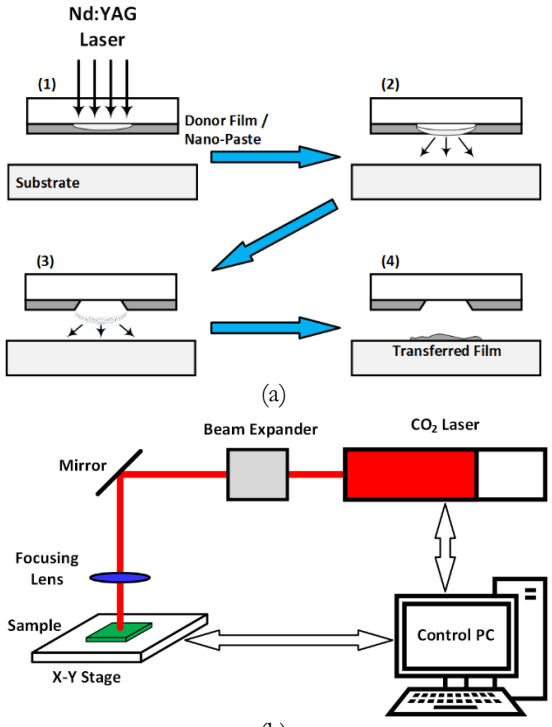

Figure (1): (a) LIFT Process and (b) LA Process.

3.Results and discussions

Fig.2 illustrates two silver-coated quartz substrates after LA using CO_2 laser beam power; P=10 W and a scanning speed, S=2 mm/sec. The samples marked (3) and (5) resulting from the LIFT process were coated using Nd:YAG laser beam; n=50 pulses and pulse energies of E=5 J and E=3J respectively.

(a) (b)

Figure (2): Silver nanofilms on quartz substrates after LA using P=10 W and S=2 mm/sec; (a) n=50 pulses, E=5 J and (b) n=50 pulses, E=3 J.

The result of this work can be classified to various categories

3.1 The Microstructure Morphology

The microstructure surface morphology of annealing metallic nano films was studied using an optical microscope. The image of an optical microscope (Fig. 3) could display the effect of power and scanning speed that used in laser annealing system.

Similarly, the microstructure of the annealed silver nano films was studied. The image shows the morphology of silver nanoparticle deposited on quartz surface by LIFT process before annealing process.

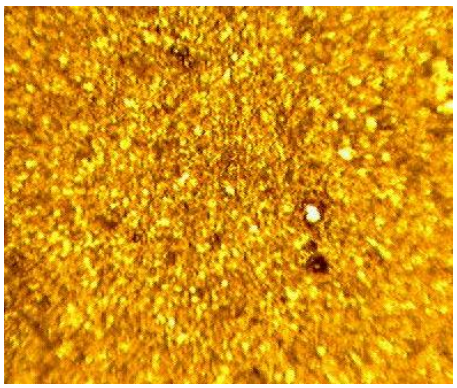

Figure (3): The surface morphology of un annealed silver nanofilm on the quartz surface.

Figure (4) shows the surface morphology of silver nanofilm prepared using E=3J pulse energy (a) n=10 pulses and (b) n=30 pulses. The two samples were annealed with P=10 W and S=2 mm/sec. The image shows in the homogenous size distribution of the silver microstructure.

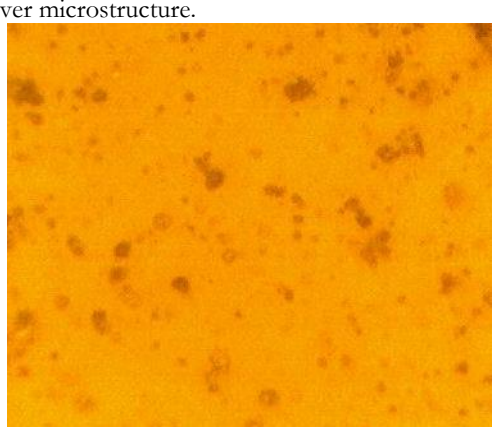

(a)200X

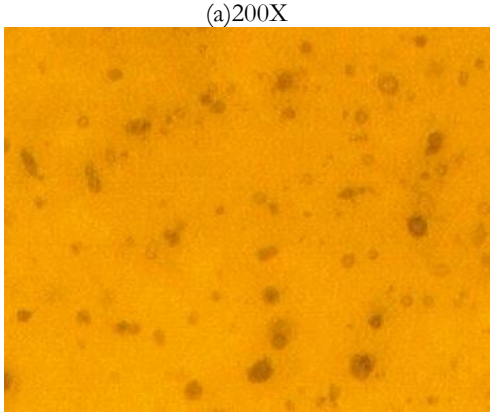

(b)200X

Figure (4): The surface morphology of annealed silver nanofilm with power 10 W and scanning speed of 2 mm/s, with no. of pulse (a)10 (b)30.

While the surface morphology of silver nanofilm prepared by LIFT process with 50 laser pulse and 3 and 5 Joule respectively, that annealed with power (10 W) and scanning speed (2 mm/sec) is shown in Fig. 5. The high density of the microstructure can be distinguished in this case.

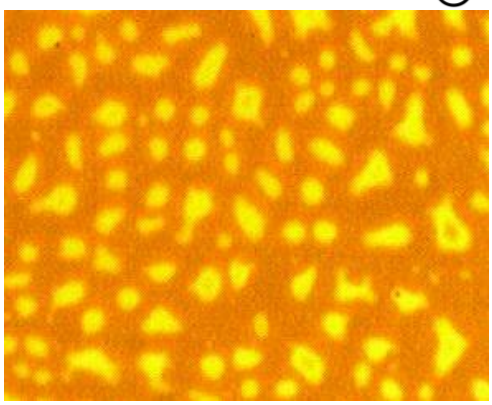

(a)200X

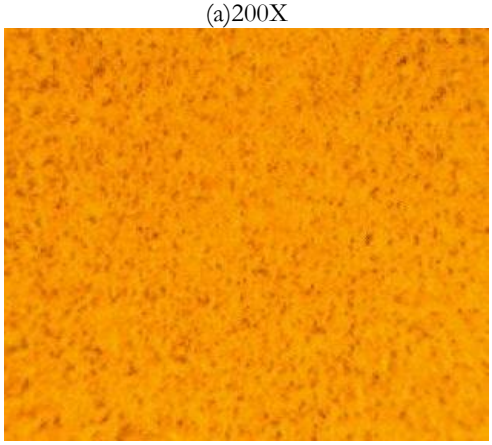

(b)200X

Figure (5): The surface morphology of annealed silver nanofilm with power 10 W and scanning speed=2 mm/s, with energy(a) 3 J (b) 5 J.

3.2The Nanostructure Morphology

The nanostructure of the silver coated quartz substrate has been identified using AFM. The AFM images show the surface morphology before and after laser annealing. Table 1. and Fig.6 show AFM images for the surface morphology of the silver film before laser annealing with particles diameter of 252 nm. While homogeneous distribution of average diameter of 60 nm and 51 nm after annealing for two film thickness Fig. 6b and 6c, respectively. The corresponding histograms represent the particle size distribution.

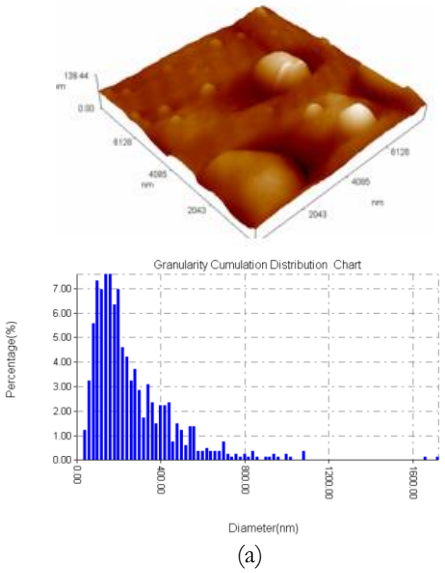

(a)

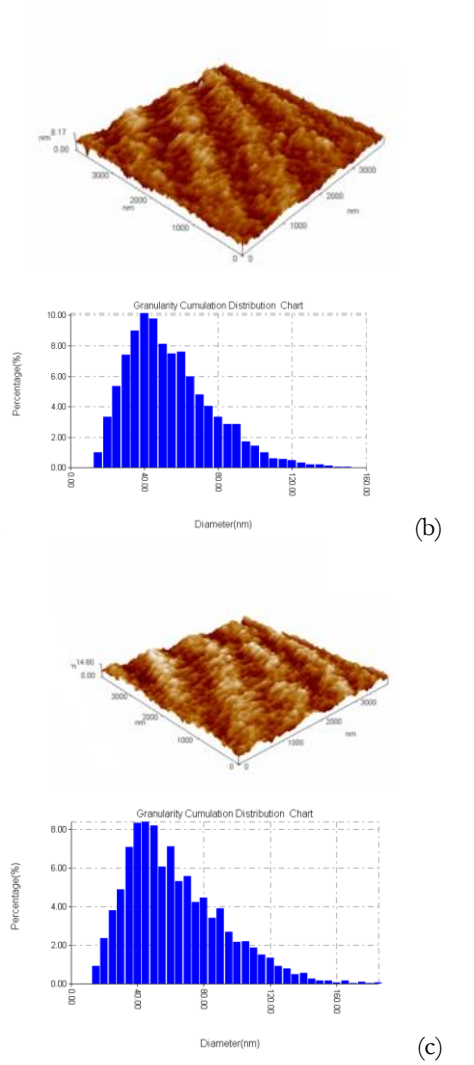

Figure (6): AFM images of silver nanofilm and corresponding size distribution (a) before and (b) (c) after annealing with no. of pulse 10 and 30 respectively.

Table (1): show the AFM different root mean square and particle average diameter.

Sample (No. of pulse)	Roughness (nm)	Average diameter (nm)
Before Annealing	10.3	252.22
After Annealing (10)	0.772	51.74
After Annealing (30)	1.76	60.60

3.3 The Optical Absorption

The optical properties of the laser annealed films were examined using diffuse reflection spectroscopy. Fig. 7(a) shows the optical absorption spectra of silver before and after nanofilm annealing. The absorption spectra reveal a small red shift at peak position are (449.25 nm) and FWHM (107.27 nm) when 10 W laser power was used for 2 mm/sec compared with (437.48 nm) and (129.26 nm) respectively before laser annealing. This could be attributed to the heating effect and recrystallization in the annealed area. While comparison between four samples of sliver nanofilm with no. of pulse (10, 30, 50 and 50) shown in Fig. 7b. Table 2 gives the experimental data of the absorption spectra. The decrease in the absorbance peak position for higher film of no. of pulse of 30 to 449.25 nm is related to the heat dissipation effect deeper inside the film and subsequent larger nano crystallite sizes.

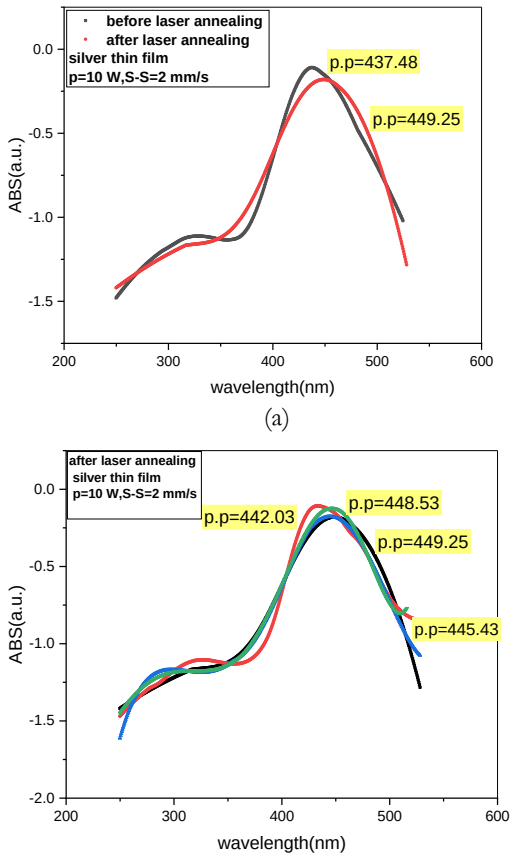

Figure (7): Comparison of optical absorption spectra before and after laser annealing of silver nanofilm with thickness (a) 20 nm (b) Comparison of optical absorption spectra after laser annealing of silver nanofilm.

Table (2): The experimental data of optical absorption spectra before and after laser annealing for silver nanofilm.

No. of pulse	Peak position		FWHM (nm)
	Before annealing(nm)	After annealing(nm)	
10	437.48	445.43	92.14
30	437.48	449.25	107.27
50	437.48	442.03	100
50	437.48	448.53	81.48

3.4 Thermal Analysis

The described model is realized in COMSOL using 3D coordinate systems a time dependent study in the application mode Heat Transfer in Solids (ht). The sample geometry is made as block with dimension of (15 mm width,15 mm depth and 1mm height) represent quartz substrate and use spheres with different radius (10 ,20,30,40 and 60 nm) to represent gold and silver nano particles that deposited on quartz surface with different interval distance as shown below(Fig 8).

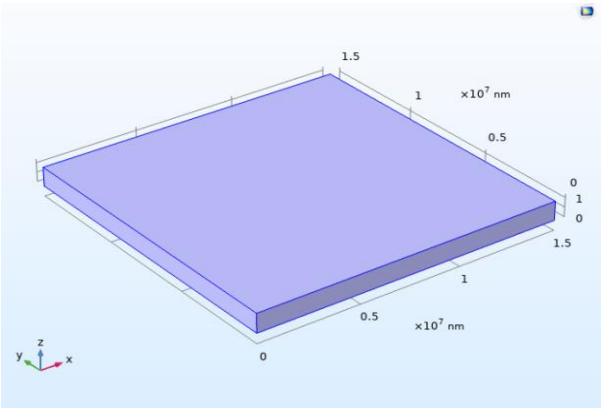

Figure (8): The structure using in COMSOL.

Then define the material taken from the COMSOL material library, so modeling the incident heat flux boundary conditions from the laser heat as a spatially distributed heat source on the surface, Let's consider a heat transfer problem where a circular heat source with a radius r is traveling in the x direction with a velocity v. Its intensity has a parabolic distribution with a peak value q_o. A mathematical description of this load could be

$$q_o = \frac{p*2}{\pi*r^2} \qquad \text{.....(1)}$$

Where the p is power laser in (W), r is spot radius in (mm), q_o is heat flux in(w/m^2) ; For a traveling load, it is obviously not possible to have domain boundaries, or even a mesh, that fits the load distribution at all times. The load distribution itself can be entered in a straightforward manner. Since the variable for the radial coordinate, r, will be used in two places, it is a good idea to define it as a variable. The entire input for the moving heat source is shown below figure 3-10 shows the flow chart of the thermal calculations.

The laser beam heating of materials depends on the laser power and scanning speed and the film thickness. To illustrate the process of heating the material and the depth of the heat affected zone, COMSOL Multiphysics software was used to study the thermal profile within the silver thin film. Various effective parameters were examined in the laser annealing process. Laser power in range (6, 8, 10) W, scanning speed in range (1, 2, 3) mm/s and different film thicknesses in range (10, 20, 30) nm were used in this study. These parameters were selected according to the experimental conditions in this work. Figure 5 illustrates the time evolution for the laser annealed silver nanofilms, while figures 6 to 8 show 3D graphs representing the maximum temperature variation with power and film thickness at each scanning speed.

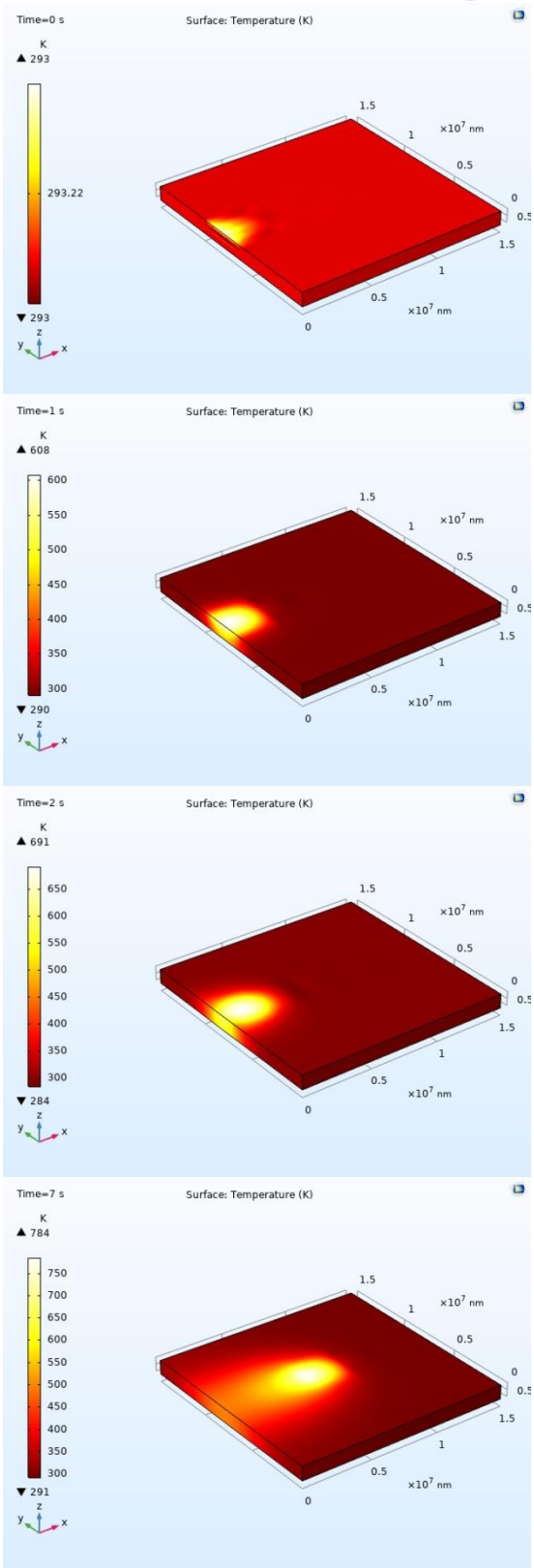

Figure (9): The surface temperature distribution for silver nanofilm annealing with thickness (20 nm) at 8 W and scanning speed 1 mm/s at 0, 1, 2, and 7 seconds respectively.

4. Conclusions

Laser annealing of silver film can be used to synthesize nanostructures. It is found that small film thickness produces homogeneous nanostructures with smaller sizes. Moreover, the optical absorption spectra

reveal small shift in the peak position due to the laser heating effect. Design of expert analysis could extremely help to understand the thermal profile at the film surface when various sets of processing parameters are used in the laser annealing process.

5. References

[1] A. Brown and B. Johnson, "Laser-induced annealing of silver nanofilms on quartz substrates: Surface morphology and plasmonic properties," *Journal of Applied Physics*, vol. 125, no. 18, p. 185302, 2019.

[2] V. K. Chaturvedi, A. Kushwaha, S. Maurya, N. Tabassum, H. Chaurasia, and M. P. Singh, "Wastewater Treatment Through Nanotechnology: Role and Prospects," in *Restoration of Wetland Ecosystem: A Trajectory Towards a Sustainable Environment*, Springer, 2020, pp. 227–247.

[3] P. M. Norris and L. E. Friedersdorf, Women in Nanotechnology: Contributions from the Atomic Level and Up. Springer, 2019.

[4] M. D. Ooms, Y. Jeyaram, and D. Sinton, "Disposable plasmonics: rapid and inexpensive large area patterning of plasmonic structures with CO_2 laser annealing," *Langmuir*, vol. 31, no. 18, pp. 5252–5258, 2015.

[5] B. Bhushan, Springer handbook of nanotechnology. Springer, 2017.

[6] X. Chen et al., "Optimization of laser annealing parameters for silver nanofilms on quartz substrates," *Applied Surface Science*, vol. 543, p. 148973, 2021.

[7] M. Ohering, Materials science of thin films deposition and structure, (2002).

[8] K. I. Mohammed, A. S. Jasim, and S. N. Rashid, "Effect of Annealing by CO_2 Laser on Structural and Optical Properties of CuO Thin Films Prepared by Sol–Gel Method," *Int J Phys*, vol. 4, no. 3, pp. 59–63, 2016.

[9] C. Garcia and E. Martinez, "Structural evolution of laser-annealed silver nanofilms on quartz," *Nanoscale Research Letters*, vol. 12, no. 1, pp. 1-8, 2017.

[10] D. Jones et al., "Tailoring plasmonic resonances in laser-annealed silver nanofilms on quartz substrates," *Optics Express*, vol. 28, no. 11, pp. 16247-16259, 2020.

[11] S. K. Maurya, Y. Uto, K. Kashihara, N. Yonekura, and T. Nakajima, "Rapid formation of nanostructures in Au films using a CO_2 laser," *Appl. Surf. Sci.*, vol. 427, pp. 961–965, 2018.

[12] K. Gupta, Surface Engineering of Modern Materials. Springer, 2020.

[13] L. Tyagi *et al.*, "Improved Absorbance and Near-Infrared Dispersion of AuGe Nanoparticles over Au Nanoparticles Prepared with Similar Thermal Annealing Environment," *Plasmonics*, vol. 13, no. 6, pp. 1947–1962, 2018.

[14] H. Nguyen, S. Arafin, J. Piao, and T. V. Cuong, "Nanostructured Optoelectronics: Materials and Devices." Hindawi, 2016.

[15] S. Lee and Y. Kim, "Applications of laser-annealed silver nanofilms on quartz in integrated photonics," *Journal of Nanophotonics*, vol. 13, no. 1, p. 016003, 2019.

[16] H. K. Lin and B. F. Chung, "Effects of thermal treatment on optoelectrical properties of AZO/Ag-Mg-Al thin films," *Appl. Surf. Sci.*, vol. 467, pp. 249–254, 2019.

[17] W. M. Abbott *et al.*, "Less is More: Improved Thermal Stability and Plasmonic Response in Au Films via the Use of SubNanometer Ti Adhesion Layers," *ACS Appl. Mater. Interfaces*, vol. 11, no. 7, pp. 7607–7614, 2019.

[18] W. Li and L. Wu, "Advanced characterization of laser-annealed silver nanofilms on quartz substrates," *Applied Physics Letters*, vol. 118, no. 8, p. 084001, 2023.

[19] J. Huang *et al.*, "Boosting the kesterite Cu2ZnSnS4 solar cells performance by diode laser annealing," *Sol. Energy Mater. Sol. Cells*, vol. 175, pp. 71–76, 2018.

[20] J. Smith et al., "Controlled growth of silver nanoparticles on quartz substrates via laser annealing," *Nanotechnology*, vol. 29, no. 18, p. 185301, 2018.

[21] K. Zimmer *et al.*, "Towards fast nanopattern fabrication by local laser annealing of block copolymer (BCP) films," *Appl. Surf. Sci.*, vol. 470, pp. 639–644, 2019.

[22] K. Tanaka and T. Yamamoto, "Stability and durability of laser-annealed silver nanofilms on quartz substrates," *ACS Applied Materials & Interfaces*, vol. 11, no. 31, pp. 28430-28437, 2019.

[23] H. Wang and M. Li, "Comparative study of laser versus thermal annealing of silver nanofilms on quartz substrates," *Journal of Physics D: Applied Physics*, vol. 51, no. 43, p. 435102, 2018.

[24] C. Wen *et al.*, "Thermal annealing performance of sulfur-hyperdoped black silicon fabricated using a Nd: YAG nanosecond-pulsed laser," *Mater. Res. Bull.*, vol. 93, pp. 238–244, 2017.

[25] Q.-Y. Wang, Y.-C. Xi, Y.-H. Zhao, S. Liu, S.-L. Bai, and Z.-D. Liu, "Effects of laser re-melting and annealing on microstructure, mechanical property and corrosion resistance of Fe-based amorphous/crystalline composite coating," *Mater. Charact.*, vol. 127, pp. 239–247, 2017.

[26] Q. Zhang et al., "Computational modeling of laser-induced annealing of silver nanofilms on quartz substrates," *Surface Science*, vol. 717, p. 121867, 2022.